analytical chemistry
Technical Note
pubs.acs.org/ac

Fourier Transform-Plasmon Waveguide Spectroscopy: A Nondestructive Multifrequency Method for Simultaneously Determining Polymer Thickness and Apparent Index of Refraction

Jonathan M. Bobbitt,[†,‡] Stephen C. Weibel,[§] Moneim Elshobaki,[⊥,#] Sumit Chaudhary,[∥,⊥] and Emily A. Smith*[,†,‡]

[†]The Ames Laboratory, U.S. Department of Energy, Ames, Iowa 50011, United States
[‡]Department of Chemistry, Iowa State University, Ames, Iowa 50011, United States
[§]GWC Technologies Inc., Madison, Wisconsin 53719, United States
[∥]Department of Electrical and Computer Engineering, Iowa State University, Ames, Iowa 50011, United States
[⊥]Department of Materials Science and Engineering, Iowa State University, Ames, Iowa 50011, United States
[#]Department of Physics, Mansoura University, Mansoura, 35516, Egypt

Supporting Information

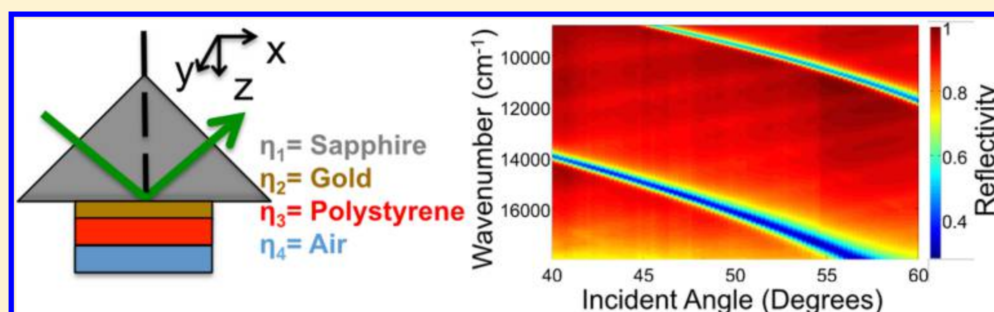

ABSTRACT: Fourier transform (FT)-plasmon waveguide resonance (PWR) spectroscopy measures light reflectivity at a waveguide interface as the incident frequency and angle are scanned. Under conditions of total internal reflection, the reflected light intensity is attenuated when the incident frequency and angle satisfy conditions for exciting surface plasmon modes in the metal as well as guided modes within the waveguide. Expanding upon the concept of two-frequency surface plasmon resonance developed by Peterlinz and Georgiadis [*Opt. Commun.* **1996**, *130*, 260], the apparent index of refraction and the thickness of a waveguide can be measured precisely and simultaneously by FT-PWR with an average percent relative error of 0.4%. Measuring reflectivity for a range of frequencies extends the analysis to a wide variety of sample compositions and thicknesses since frequencies with the maximum attenuation can be selected to optimize the analysis. Additionally, the ability to measure reflectivity curves with both p- and s-polarized light provides anisotropic indices of refraction. FT-PWR is demonstrated using polystyrene waveguides of varying thickness, and the validity of FT-PWR measurements are verified by comparing the results to data from profilometry and atomic force microscopy (AFM).

Spectroscopies based on reflection from an interface, such as surface plasmon resonance (SPR) and plasmon waveguide resonance (PWR), have many applications including monitoring biomolecule interactions and materials characterization.[1−4] In a typical SPR experiment, the reflected light intensity is measured from a prism/thin noble metal film interface. Under conditions of total internal reflection, the reflected light intensity is attenuated when surface plasmons are excited in the smooth metal film. The resonant conditions are susceptible to slight changes in the index of refraction of the layer adjacent to the metallic film, making SPR quite sensitive.[5,6] In a PWR experiment, the reflected light intensity is recorded at a prism/noble metal film/waveguide interface (Figure 1). A dielectric material will function as a waveguide when its thickness is greater than $\sim\lambda/2\eta$ where λ is the wavelength of light and η is the dielectric's index of refraction. Under total internal reflection, surface plasmons in the noble metal film as well as

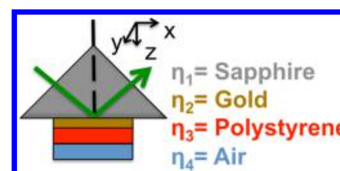

Figure 1. Representative sample setup for a FT-PWR experiment.

Received: August 19, 2014
Accepted: November 20, 2014
Published: November 20, 2014

ACS Publications © 2014 American Chemical Society

the guided modes in the dielectric material can be excited at certain angles. PWR reflectivity curves are narrower than SPR reflectivity curves due to the electromagnetic field within the dielectric material having a greater propagation distance. This leads to better sensitivity for PWR than SPR.[7] Both p- and s-polarized light can be used to excite guided modes in PWR, which enables anisotropic properties to be measured.[8,9]

SPR measurements with a single excitation frequency are capable of determining absorbate thickness or the dielectric constant but not both parameters simultaneously. Peterlinz et al. developed a method using two frequencies of light to determine both parameters concurrently without the need to change solvents.[10] The method works by determining the continuum solution to eq 1 at two incident frequencies, where k is the plasmon wave vector, η is the index of refraction for the analyte layer, and d is the thickness of the analyte layer.

$$k = \eta \times d \quad (1)$$

Peterlinz et al. termed the continuum solutions trial curves.[10] In theory, using more than two frequencies provides a more accurate determination of the intersection point of the trial curves, thus providing a more accurate apparent index of refraction and thickness of the analyte layer. A three frequency analysis has been reported for thin films as well as waveguides.[11]

A white light source can be used to scan through a range of frequencies at a fixed incident angle to generate reflectivity curves. This has been demonstrated for SPR.[12−14] However, to the best of our knowledge, no frequency scanning technique has been used with a PWR substrate to measure absorbate thickness and dielectric constant. The sensitivity of a frequency scanning SPR technique increases as lower frequencies are used.[14] Frutos et al. demonstrated the advantages of using frequencies in the infrared region below 3.3×10^{14} Hz with a Fourier transform (FT)-SPR spectrometer.[15] More recently, FT-SPR has been used in biological studies, to monitor polyelectrolyte multilayer assembly and nonspecific and specific interactions on functionalized polymer surfaces and to study sputtered indium tin oxide film deposition characteristics.[16−24]

Herein, we describe the technique FT-PWR for simultaneous measurements of apparent index of refraction and thickness using narrow reflectivity curves. This work combines the multiplexing capabilities of FT to perform a multifrequency analyses. FT-PWR offers the flexibility of selecting frequencies of interest to the user or frequencies that produce the greatest attenuation of the reflectivity for a given sample and is less costly with respect to time and money compared to an instrument with multiple, single-frequency sources. There is an increasing demand for nondestructive techniques to measure optical properties of thin films, such as those found in sensors, organic solar cells, catalytic films, lithographically produced electronics, and coatings for biomedical applications. FT-PWR is a nondestructive technique capable of determining this information.

MATERIALS AND METHODS

Sample Preparation. The gold films were supplied by GWC Technologies Inc., Madison, WI, or fabricated at Oak Ridge National Laboratory's Center for Nanophase Materials Sciences, Oak Ridge, TN. A Ti adhesion layer (2 nm) and Au layer (50 ± 5 nm) were deposited onto a 25.4 mm diameter sapphire disk (Meller Optics, Providence, RI). After the deposition, the slides were washed with 2-propanol (Fisher Scientific, Waltham, MA) and dried with nitrogen gas. An 8.48, 8.27, 6.48, and 5.47 wt % polystyrene (Sigma-Aldrich, St. Louis, MO) in toluene (Fisher Scientific, Waltham, MA) solution was prepared. The films were prepared by spin coating 200 μL of polystyrene solution onto the gold films using a KW-4A spin coater (Chemat Technology, Northridge, CA) at 3000 rpm for 60 s.[25] The polystyrene solutions were also spin coated onto 25 mm square glass coverslips (Corning Inc., Corning, NY) to determine an average thickness by the NewView 7100 Profilometer (Zygo, Middlefield, CT). A Veeco Digital Instruments atomic force microscope (AFM) was used to measure the thickness of the FT-PWR films. The films were scratched using a sharp needle, and the resulting profile was scanned at scan rate and size of 0.1 Hz and 170 μm × 5 μm, respectively.

Instrumentation and FT-PWR Measurements. FT-PWR data were collected on the SPR100, which is an integrated system developed by GWC Technologies, Inc. A Thermo Nexus FT-IR (Thermo Fisher Scientific Inc., Waltham, Ma) consisting of a tungsten lamp, a calcium fluoride beamsplitter, and an external collimated beam coupled to a FT-SPR module (GWC Technologies, Inc.). The module has beam shaping optics (telescope design), a silicon detector, and a motorized rotation stage. Reflectivity was measured from 18 000 to 8800 cm^{-1} while the incident angle was scanned from 36 to 60°. The FT-PWR measurements were an average of 32 scans with a 32 cm^{-1} resolution and an incident angle resolution of 0.25°. Reported incident angles were corrected for the refraction within the prism using Snell's law, and experimental reflectivity curves were shifted by 0.95° to match the calculated reflectivity curves.

Calculated Reflectivity Curves. The reflected light was modeled by Fresnel calculations as outlined by Hansen using in-house developed programs.[26] All calculations were performed over an angular range of 0.00° to 90.00° with a resolution of 0.01°. Indices of refraction from the literature at specified frequencies were used to develop a fit equation to extrapolate to values at other frequencies for sapphire,[27] water,[28] and polystyrene.[29] The complex indices of refraction for the gold films used in this study were determined by fitting experimental data, as shown in Figure S1, Supporting Information. The real (η_{Au}) and imaginary (k_{Au}) indices of refraction at 6 wavenumbers were fit to a polynomial or linear function, respectively (Figure S2, Supporting Information). The equations for η_{Au} and k_{Au} are presented in eqs 2 and 3, where $\tilde{\nu}$ represents the wavenumber of light.

$$\eta_{Au} = 1.259 \times 10^{-8}\tilde{\nu}^2 - 3.270 \times 10^{-4}\tilde{\nu} + 2.248 \quad (2)$$

$$k_{Au} = 17.32 - 9.292 \times 10^{-4}\tilde{\nu} \quad (3)$$

Equations 2 and 3 were used to calculate values at other frequencies above 14 924 cm^{-1}. These fit functions qualitatively agree with values found in the literature over the range of 14 286 to 9091 cm^{-1}.[30] The index of refraction used for air was 1.00 over the entire frequency range.[31]

Data Analysis. The FT-PWR data consists of reflectivity values at a range of incident frequencies and angles. In order to determine the angle of maximum attenuation at a selected wavenumber, a 2.55° region of the experimental FT-PWR reflectivity curve was fit to a Voigt profile using the "Multipeak fitting 2" algorithm in IGOR Pro 6.34A. The Voigt function, a combination of Gaussian and Lorentzian, produced the smallest residual.

The polystyrene thickness (d) versus index of refraction (η) curves, hereafter called trial curves, were constructed by fitting the reflectivity as a function of incident angle and fixed frequency using Fresnel reflectivity coefficients. The index of refraction was varied from 1.55 to 1.80 in 0.05 increments (unless otherwise noted), and the thickness was optimized until the experimental and calculated maximum attenuation were within ±0.001°. The goal of the analysis was to determine the intersection point(s) from among all the trial curves generated for selected wavenumbers. Since the index of refraction is wavenumber dependent, trial curves have to be adjusted for dispersion and compared to a single reference wavenumber. The *wavelength* dependence of a transparent material's index of refraction in the visible and near-infrared regions follows Cauchy's equation.[29] Eq 4 represents the fit to Cauchy's equation in units of wavenumbers for polystyrene's index of refraction. The dispersion was calculated by taking the derivative of eq 4 as shown in eq 5. The dispersion adjustment for the nonreference wavenumbers were calculated using eq 6. In eq 6, $\tilde{\nu}_2$ represents the reference wavenumber and $\tilde{\nu}_1$ represents the wavenumber for the trial curve being adjusted for dispersion.

$$\eta(\tilde{\nu}) = 1.563 + 1.000 \times 10^{-10}\tilde{\nu}^2 - 6.471 \times 10^{-21}\tilde{\nu}^4 \quad (4)$$

$$\frac{d\eta}{d\tilde{\nu}} = 2.000 \times 10^{-10}\tilde{\nu} - 2.588 \times 10^{-20}\tilde{\nu}^3 \quad (5)$$

$$\eta(\tilde{\nu}_2) = \eta(\tilde{\nu}_1) + \frac{d\eta}{d\tilde{\nu}} \times (\tilde{\nu}_2 - \tilde{\nu}_1) \quad (6)$$

Once adjusted for dispersion, all trial curves were fit to an offset exponential function unless otherwise stated. The intersection point of the fit functions was found using the fsolve function in MATLAB R2014a (The MathWorks, Inc., Natick, MA).

■ RESULTS AND DISCUSSION

FT-PWR Measurements of Polystyrene Waveguides. The purpose of this work is to demonstrate the FT-PWR technique and its use to accurately measure both the thickness and an apparent index of refraction of polymer waveguides. A polymer film of sufficient thickness will act as a waveguide. The minimum polystyrene thickness required to form a waveguide is ~360 nm for 8803 cm^{-1} incident light and ~175 nm for 17989 cm^{-1}. The frequency and angle where the reflected light intensity is attenuated when a waveguide-supporting film is coated on a plasmon-supporting film depends on the waveguide thickness. More than one waveguide mode may be excited, and attenuation of the reflected light may occur at multiple frequencies and angles. Figure 2A,B shows the p-polarized light reflectivity plots for two polystyrene films coated on a 50 nm gold film. The polystyrene films were prepared by spin coating an 8.27 (Figure 2A) or 6.48 (Figure 2B) wt % polystyrene solution onto the gold film. As measured by profilometry, the thicknesses are 690 ± 40 and 450 ± 20 nm for the 8.27 and 6.48 wt % films, respectively. The 690 ± 40 nm polystyrene waveguide has two distinct FT-PWR peaks represented by the blue areas of the plot. These correspond to two waveguide modes. The 450 ± 20 nm polystyrene waveguide has one distinct FT-PWR peak. The surface plasmon mode is not measured for any of the films due to the angle range of the instrument (36° to 60°). The SPR angle at 14 000 cm^{-1} is calculated to be 72.30° and 73.13° for polystyrene films

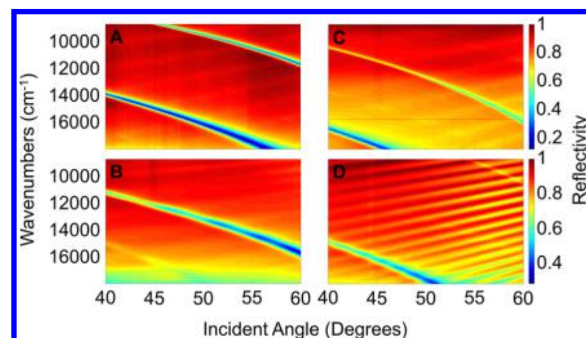

Figure 2. Experimental FT-PWR reflectivity plots of a (A, C) 8.27 wt % and (B, D) 6.48 wt % polystyrene waveguide. A and B were collected with p-polarized light and C and D with s-polarized light.

with thicknesses of 450 and 690 nm, respectively. The FT-PWR plots provide more information than measurements collected with a fixed frequency or incident angle. For example, at certain incident frequencies, no attenuation of the reflected light is measured at this incident angle range. If using a fixed frequency source, there is a limited range of waveguide thicknesses that can be measured.

FT-PWR can be used to measure reflectivity of both p- and s-polarized light. Figure 2C,D shows the s-polarized FT-PWR plots for the 690 ± 40 and 450 ± 20 nm polystyrene films, respectively. The s-polarized FT-PWR peaks in Figure 2C,D have a full width at half-maximum (fwhm) of 0.39° ± 0.03° (13 585 cm^{-1}) and 0.65° ± 0.03° (15 828 cm^{-1}).These are generally smaller than the fwhm values for similar waveguide modes generated with p-polarized light, 0.70° ± 0.03° (13 585 cm^{-1}) and 1.05° ± 0.05° (15 828 cm^{-1}), respectively. Fresnel reflectivity calculations for the above frequencies (13 585 and 15 828 cm^{-1}) using a 0.001° angle resolution follow the same trend as the experimental results. For 13 585 and 15 828 cm^{-1}, the calculated differences in the fwhm for the p- and s-polarized FT-PWR peak are 0.310° and 0.400°, respectively. Smaller fwhm can lead to better detection limits and higher precision with sufficient experimental angular and/or spectral resolution.

The faint peak starting at 15 020 cm^{-1} and 40° in the bottom of Figure 2B has the same characteristics as the more prominent peak in Figure 2D and is the result of the polarizer leaking s-polarized light when set to p-polarization. The data collected with s-polarized light occasionally had a fringe pattern throughout the plot (Figure 2D), which requires further exploration to explain.

FT-PWR Multifrequency Analysis to Measure Waveguide Thickness and Apparent Index of Refraction. In order to use FT-PWR to measure the thickness and apparent index of refraction of the waveguide layer, accurate optical properties at a range of frequencies for all other interfacial layers must be known. A thin gold films' optical properties may vary depending on preparation conditions. In order to minimize error in the analysis, the index of refraction was experimentally measured as reported in the Supporting Information for a gold film prepared at the same time as the films used in subsequent studies.

FT-PWR measurements of waveguide thickness and apparent index of refraction start with the construction of trial curves. One trial curve is constructed for each wavenumber. FT-PWR makes it possible to construct trial curves for many wavenumbers or at selected optimal wavenumbers of maximum attenuation, which may increase precision compared

to the use of two or three fixed frequency sources that may not be ideal for a given sample. Trial curves are constructed for three polystyrene waveguides at three selected wavenumbers with the greatest attenuation across the range of 8803 to 17 989 cm^{-1}. Figure 3 shows the trial curves for 6.48 (A), 8.27 (B), and

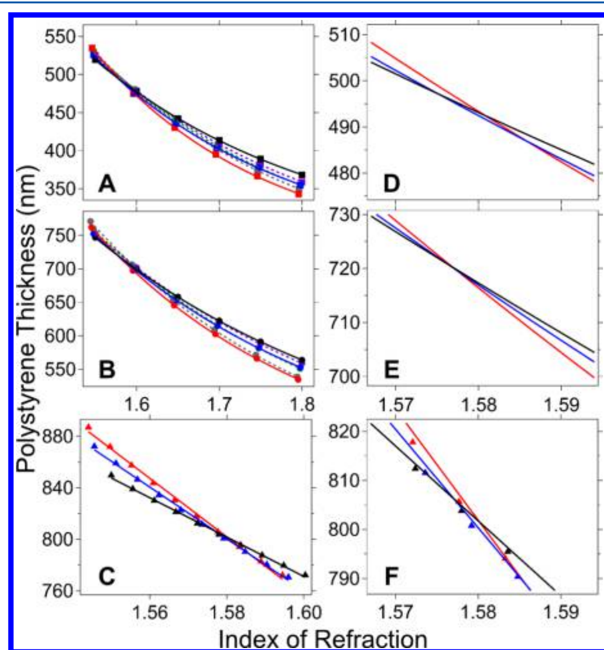

Figure 3. Trial curves for (A) 6.48, (B) 8.27, and (C) 8.48 wt % polystyrene waveguides where the lines represent the offset exponential fits in (A) and (B) and linear fits in (C) for p-polarized (solid) and s-polarized (dashed) light. (A) 17 419 cm^{-1} (gray), 16 832 cm^{-1} (green), 16 316 cm^{-1} (purple), 14 571 cm^{-1} (red), 13 622 cm^{-1} (blue), and 12 590 cm^{-1} (black). (B) 17 665 cm^{-1} (gray), 16 524 cm^{-1} (green), 15 828 cm^{-1} (purple), 15 606 cm^{-1} (red), 14 395 cm^{-1} (blue), and 13 585 cm^{-1} (black). (C) 17 094 cm^{-1} (red), 16 399 cm^{-1} (blue), and 14 680 cm^{-1} (black). D, E, and F are an expanded view of A, B, and C that show the intersection points for p-polarized light trial curves.

8.48 (C) wt % polystyrene waveguides. The solid lines indicate trial curves for p-polarized light, and the dashed lines in A and B are the trial curves from s-polarized light. The trial curves were constructed using 6 indices of refraction ranging from 1.5 to 1.8 and a best-fit offset exponential function defined from these points. The intersection of the trial curves represents the solution for the waveguide thickness and apparent index of refraction. The thicknesses are 495 ± 3 and 720.4 ± 0.3 for the polystyrene waveguides in Figure 3A–B, respectively.

Precision in the determination of polymer thickness using 10 points to construct the trial curves was tested over a 1.55 to 1.60 range of indices of refraction (Figure 3C). The thickness determined over the larger 1.5 to 1.8 range of indices of refraction for the 8.48 wt % polystyrene waveguide was 803 ± 3 nm. The thickness was 804 ± 3 nm using the narrower 1.55 to 1.60 range of indices of refraction, indicating the precision is not improved compared to the analysis with a larger range of indices of refraction.

The addition of a fourth or fifth trial curve has no significant effect on the precision of the analysis. For the 6.48 wt % polystyrene waveguide, the thickness measured using 3 trial curves is 521 ± 6 nm. Adding a fourth trial curve corresponding to 13 560 cm^{-1} gave a thickness of 524 ± 6 nm and a fifth trial curve corresponding to 12 621 cm^{-1} gave a thickness that is not statistically different than the value obtained using 3 or 4 trial curves (525 ± 5 nm). The same result was found for the 8.48 wt % polystyrene waveguide.

Another consideration that will affect the analysis is determining the appropriate frequencies to construct the trial curves. Trial curves should be constructed using frequencies that produce the maximum attenuation in the reflected light intensity. This is demonstrated with trial curves constructed using three wavenumbers (12 612, 13 000, and 13 530 cm^{-1}) that did not show significant attenuation (i.e., reflectivities in the range of 0.6 to 0.8) for the 8.48 wt % polystyrene waveguide. The thickness measured with these trial curves is 810 ± 10 nm. This is statistically similar to the thickness measured using curves generated at wavenumbers where the reflectivity was between 0.1 and 0.3 (Table 1), yet the

Table 1. Thickness Measured by FT-PWR and Profilometry and the Percent Difference between the Two Techniques for the Indicated Polystyrene Waveguide

wt % PS	FT-PWR thickness (nm)	profilometry thickness (nm)	% difference FT-PWR and profilometry
5.47% PS P-pol Light	361 ± 2	330 ± 20	9
6.48%[a] PS P-pol Light	495 ± 3	450 ± 20	9
6.48% PS S-pol Light	489.4 ± 0.9		9
6.48%[a] PS P-pol Light	521 ± 6	470 ± 40	10
8.27% PS P-pol Light	720.4 ± 0.3	690 ± 40	4
8.27% PS S-pol Light	711 ± 2		3
8.48% PS P-pol Light	803 ± 3	780 ± 60	3

[a]Different polystyrene waveguides prepared using the same conditions.

uncertainty increased over three times when the trial curves are not constructed using wavenumbers with maximum attenuation. If the frequencies selected to construct the trial curves have an angle of maximum attenuation that is separated by less than 1.5°, the trial curves do not intersect. Compared to reflectivity measurements with fixed-frequency sources, the main benefit of FT-PWR is the ability to select optimal frequencies, which is a sample dependent property.

Table 1 reports the thicknesses obtained from FT-PWR and profilometry for 5 polystyrene waveguides. The average percent difference between the two measurements is 7%, and the greatest difference is with the thinner films. For the same sample and FT-PWR measurements, the percent relative error is smaller using s-polarized excitation compared to p-polarized excitation. Furthermore, the profilometer consistently measured thicknesses that are less than the FT-PWR method. The thicknesses obtained by FT-PWR and profilometry are not performed on the same samples since the gold film affected the profilometry measurements. Selected polystyrene waveguides measured by FT-PWR were also measured by AFM; these values are statistically similar to the values determined by profilometry for samples prepared on a glass slide but otherwise had identical sample preparation methods. Reproducibility of the spin coater and different substrate compositions did not

dx.doi.org/10.1021/ac504103g | Anal. Chem. 2014, 86, 11957−11961

contribute to the percent differences measured by FT-PWR and profilometry. In order to obtain thicknesses using profilometry or AFM, the polystyrene film has to be scratched away. The lower thicknesses measured by profilometry and AFM could be the result of polymer remaining on the substrate after scratching the surface. The ability to obtain thicknesses from the FT-PWR analysis depends on the accuracy of the index of refraction values used to model the data as already explained.

Comparing the apparent index of refraction at the same frequency for p- versus s-polarized light provides information on anisotropic properties. For the 8.27 wt % polystyrene waveguide, the p- and s-polarized light provide statistically different indices of refraction at 15 828 cm^{-1}: 1.580 ± 0.002 for p-polarized light and 1.591 ± 0.003 for s-polarized light. Similarly, 13 585 cm^{-1} gave values of 1.5767 ± 0.0004 for p-polarized light and 1.5848 ± 0.0009 for s-polarized light. The differences between indices of refraction for p- and s-polarized light indicate the polystyrene film is anisotropic. Stress birefringence as a result of film preparation conditions may explain this.[32] The thinner 6.48 wt % polystyrene waveguide had statistically similar indices of refraction for p- and s-polarized light indicating the anisotropy is thickness dependent.

CONCLUSIONS

FT-PWR is a nondestructive technique capable of providing the apparent anisotropic indices of refraction and thicknesses for a dielectric waveguide layer suitable for total internal reflection. This technique provides better precision in determining polystyrene thickness compared to techniques like profilometry, while still maintaining the integrity of the polystyrene waveguide. FT-PWR analyses are not limited to polymer films. For example, the polystyrene layer can be replaced with a silica waveguide layer. Monitoring adsorption to the silica surface, or a modified silica surface, should be possible using FT-PWR. It is expected that FT-PWR can be used to quantify and detect anisotropic analytes at low concentrations when adsorbed to a waveguide interface and will be useful as a label free sensor for many applications.

ASSOCIATED CONTENT

Supporting Information

Additional information as noted in text. This material is available free of charge via the Internet at http://pubs.acs.org.

AUTHOR INFORMATION

Corresponding Author

*E-mail: esmith1@iastate.edu.

Notes

The authors declare no competing financial interest.

ACKNOWLEDGMENTS

This research is supported by the U.S. Department of Energy, Office of Basic Energy Sciences, Division of Chemical Sciences, Geosciences, and Biosciences through the Ames Laboratory. The Ames Laboratory is operated for the U.S. Department of Energy by Iowa State University under Contract No. DE-AC02-07CH11358. Gold film fabrication was conducted at the Center for Nanophase Materials Sciences, which is a DOE Office of Science User Facility. The authors thank Mr. Wyman Martinek (Iowa State University, College of Engineering) for allowing the use of the NewView 7100 Profilometer for thickness measurements.

REFERENCES

(1) Shumaker-Parry, J. S.; Campbell, C. T. *Anal. Chem.* **2004**, *76*, 907−917.
(2) Alves, I. D.; Park, C. K.; Hruby, V. J. *Curr. Protein Pept. Sci.* **2005**, *6*, 293−312.
(3) Huang, H.; Chen, Y. *Biosens. Bioelectron.* **2006**, *22*, 644−648.
(4) Beusink, J. B.; Lokate, A. M.; Besselink, G. A.; Pruijn, G. J.; Schasfoort, R. B. *Biosens. Bioelectron.* **2008**, *23*, 839−844.
(5) Karl, D.; Pavey, C. J. O. *Biomaterials* **1999**, *20*, 885−890.
(6) Rothenhausler, B.; Knoll, W. *Nature* **1988**, *332*, 615−617.
(7) Byard, C. L.; Han, X.; Mendes, S. B. *Anal. Chem.* **2012**, *84*, 9762−9767.
(8) Hruby, V. J.; Alves, I.; Cowell, S.; Salamon, Z.; Tollin, G. *Life Sci.* **2010**, *86*, 569−574.
(9) Harte, E.; Maalouli, N.; Shalabney, A.; Texier, E.; Berthelot, K.; Lecomte, S.; Alves, I. D. *Chem. Commun.* **2014**, *50*, 4168−4171.
(10) Peterlinz, K. A.; Georgiadis, R. *Opt. Commun.* **1996**, *130*, 260−266.
(11) Granqvist, N.; Liang, H.; Laurila, T.; Sadowski, J.; Yliperttula, M.; Viitala, T. *Langmuir* **2013**, *29*, 8561−8571.
(12) Aldinger, U.; Pfeifer, P.; Schwotzer, G.; Steinrücke, P. *Sens. Actuators, B* **1998**, *51*, 298−304.
(13) Johnston, K. S.; Mar, M.; Yee, S. S. *Sens. Actuators, B* **1999**, *54*, 57−65.
(14) Homola, J. *Sens. Actuators, B* **1997**, *41*, 207−211.
(15) Frutos, A. G.; Weibel, S. C.; Corn, R. M. *Anal. Chem.* **1999**, *71*, 3935−3940.
(16) Arena, G.; Contino, A.; D'Agata, R.; Sgarlata, C.; Spoto, G. *New J. Chem.* **2005**, *29*, 1393.
(17) Ziblat, R.; Lirtsman, V.; Davidov, D.; Aroeti, B. *Biophys. J.* **2006**, *90*, 2592−2599.
(18) Lee, H. J.; Wark, A. W.; Corn, R. M. *J. Phys.: Condens. Matter* **2007**, *19*, 375107.
(19) Lirtsman, V.; Golosovsky, M.; Davidov, D. *J. Appl. Phys.* **2008**, *103*, 014702.
(20) Boddohi, S.; Killingsworth, C. E.; Kipper, M. J. *Biomacromolecules* **2008**, *9*, 2021−2028.
(21) Boujday, S.; Methivier, C.; Beccard, B.; Pradier, C. M. *Anal. Biochem.* **2009**, *387*, 194−201.
(22) Almodovar, J.; Place, L. W.; Gogolski, J.; Erickson, K.; Kipper, M. J. *Biomacromolecules* **2011**, *12*, 2755−2765.
(23) Wei, J.; Yan, L.; Hu, X.; Chen, X.; Huang, Y.; Jing, X. *Colloids Surf., B: Biointerfaces* **2011**, *83*, 220−228.
(24) Losego, M. D.; Efremenko, A. Y.; Rhodes, C. L.; Cerruti, M. G.; Franzen, S.; Maria, J.-P. *J. Appl. Phys.* **2009**, *106*, 024903.
(25) Meyer, M. W.; McKee, K. J.; Nguyen, V. H. T.; Smith, E. A. *J. Phys. Chem. C* **2012**, *116*, 24987−24992.
(26) Hansen, W. N. *J. Opt. Soc. Am.* **1968**, *58*, 380−390.
(27) Bass, M.; DeCusatis, C.; Enoch, J.; Lakshminarayanan, V.; Li, G.; MacDonald, C.; Mahajan, V.; Van Stryland, E. *Handbook of Optics*, Third ed.; McGraw-Hill: New York, 2009; Vol. *IV*: Optical Properties of Materials, Nonlinear Optics, Quantum Optics (set).
(28) Daimon, M.; Masumura, A. *Appl. Opt.* **2007**, *46*, 3811−3820.
(29) Kasarova, S. N.; Sultanova, N. G.; Ivanov, C. D.; Nikolov, I. D. *Opt. Mater.* **2007**, *29*, 1481−1490.
(30) Johnson, P. B.; Christy, R. W. *Phys. Rev. B* **1972**, *6*, 4370−4379.
(31) Ciddor, P. E. *Appl. Opt.* **1996**, *35*, 1566−1573.
(32) Mark, H. F.; Bikales, N.; Kroschwitz, J. I. *Encyclopedia of Polymer Science and Engineering, Styrene Polymers to Toys*; Wiley: Hoboken, New Jersey, 1989.